Dalton Transactions

Accepted Manuscript

This article can be cited before page numbers have been issued, to do this please use: M. Duraiyarasu, P. Selvaraj and M. Ramasamy, *Dalton Trans.*, 2017, DOI: 10.1039/C7DT01895A.

ROYAL SOCIETY OF CHEMISTRY

rsc.li/dalton

View Article Online
DOI: 10.1039/C7DT01895A

Submitted to : Dalton Trans. (Revised)

Manuscript ID: DT-ART-05-2017-001895.R1

Copper(II)-Benzimidazole Complexes as an Efficient Fluorescent Probe for L-Cysteine in Water

Duraiyarasu Maheshwaran, Selvarasu Priyanga and Ramasamy Mayilmurugan*

Bioinorganic Chemistry Laboratory/Physical Chemistry, School of Chemistry, Madurai Kamaraj University, Madurai 625 021, Tamil Nadu, India.

*E-mail: mayilmurugan.chem@mkuniversity.org / ramamayil@gmail.com

Abstract: The copper(II) complexes $[Cu(L1)(H_2O)_2](SO_3CF_3)_2$ **1** and $[Cu(L2)(H_2O)_2](SO_3CF_3)_2$ **2** based on 2,6-bis(benzimidazolyl)pyridine have been synthesized and reported as highly selective "turn-on" optical probe for L-cysteine. The Cu(II)/Cu(I) redox potential of the probe **1** (0.14 V vs NHE) is lower than of **2 (**0.233 V vs NHE) in water. The molecular structure of **2** adopts square pyramidal geometry (τ = 0.2545) and its Cu-N_{py} bond (1.958 Å) of middle pyridine is shorter than other two Cu-N_{benzim} bonds (Cu-N, 1.995, 2.000 Å). The axial Cu-O2 bond distance (2.247 Å) is slightly longer than the equatorial Cu-O1 bond distance (1.953 Å). The square based geometry is further supported by $A_{\|}$ value of 156×10^{-4} cm^{-1} in EPR at 70 K. The d-d and ligand-based transitions appear at 662 and 314-356 nm for **1** and 651 and 313-360 nm for **2** respectively in HEPES buffer at pH 7.34. These probes showed a selective and efficient "turn-on" fluorescence behavior towards Cys over other natural amino acids with the binding constant (**1**, 5.4×10^4; **2**, 1.30×10^4) with a limit of detection 2.9×10^{-8} M and 3.32×10^{-8} M respectively at pH, 7.34. The quantum yield for the detection of Cys by **1 (**14.7%) is much lower than by **2** (23%). The fluorescence intensity of **1** and **2** have been also slightly enhanced by histidine but it is relatively lower than that of exhibited by Cys.

View Article Online
DOI: 10.1039/C7DT01895A

Introduction

Amino acids play an important role in biological systems, among the twenty amino acids, cysteine is acting as powerful detoxifiers and active site for several metalloenzymes in the body fluids.[1] Also, it involves in maintain critical metabolic functions by acting as intracellular redox buffer.[2] The change in the level of Cys causes oxidative damage, hematopoiesis, psoriasis, leukocyte loss, metabolic disorder, cardiovascular and Alzheimer's disease.[3] Moreover, the protease family enzymes cysteine cathepsins are translocated into the cell surface and involving degradation of extracellular matrix (ECM) leading to malignant cell growth.[4] Thus, abnormal level of this amino acids is indicating a variety of diseases such as chronic kidney disease, hematopoiesis decrease, leucocyte loss, psoriasis, pulmonary diseases, stress, psychological disorders, etc.[5] The level of amino acid Cys has to be determined to avoid such complications. So the detection of amino acid can be developed by various methods such as spectroscopic, chromatographic and electrochemical methods.[5c,5d,6]

Several chemodosimetric sensors have been reported for detecting thiol containing compounds (Cys, Hcy, GSH) without selectivity.[5b, 7] However, only a limited reports are available on Cu^{2+}-based probes which include anthracene, coumarin, a zwitterionic chromophore, fluorescein and other fluorophores for detecting amino acids (Histidine, Cys, Hcy) and GSH without selectively.[8] Very recently, we have developed a copper(II)-based probe for Cys detection with an excellent limit of detection and selective.[9] These Cu^{2+}-based probes have received much attention as 'turn-on' fluorescence probes owing to its tunable 'Off-On' signaling property.[8] Due to its intrinsic paramagnetic property of Cu^{2+} (d^9) which tend to quench the fluorescence intensity of ligand to "off state" on complexation.[10] The soft S-donor nucleophile in Cys has preferable tendency for the coordination with Cu^{2+} and subsequently reduced into Cu^{+}.[8] In this report, we have synthesized and studied Cu^{2+}-probes based on 2,6-bis(benzimidazolyl)pyridine as 'turn-on' fluorescent probe for L-Cysteine. This probing mechanism has established by spectral, redox and geometrical changes by DFT studies on interaction with amino acid Cys. The ligand 2,6-bis(benzimidazolyl)pyridine has a very similar ligand architecture to our previously reported terpyridine-based ligand and two benzimidazole arms replaces pyridine arms.[11] Previously, the Cu(II), Zn(II, Au(III) and lanthanides coordination complexes of this tridentate ligand have been extensively studied[12-16] for DNA interaction and

View Article Online
DOI: 10.1039/C7DT01895A

validation with cancer cells, detection of copper(II) ions and detection of pyrophosphate.[17] However none these studies focused on detection of biomaterials and metabolites.

Results and Discussion

Synthesis and characterization: The ligands L1 and L2 were synthesized according to the previously published method[11] by the reaction of a 2,6-pyridine-dicarboxylic acid and 1,2-diaminobenzene in the presence of polyphosphoric acid (PPA) at 230 °C under nitrogen. The methylation of L1 using methyl iodide in the presence of KOH in acetone results the formation of L2 and it is characterized by NMR and ESI-MS (*m/z*, 340.44). The copper(II) complexes have been isolated as green solid by the reaction of $Cu(SO_3CF_3)_2$ with ligands L1 and L2 in methanol at 55 °C. The formation of complexes was confirmed by HR-ESI-MS and formulated as $[Cu(L1)(H_2O)_2](SO_3CF_3)_2$ **1** and $[Cu(L2)(H_2O)_2](SO_3CF_3)_2$ **2** (Figure S1). This is further supported by the single crystal X-ray structure of **2**. The suitable single crystal of **2** for X-ray diffraction has been grown in the acetonitrile-water mixture by slow evaporation at room temperature.

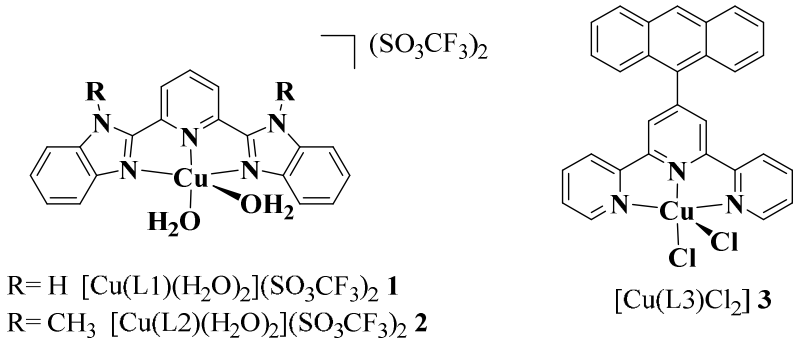

R= H $[Cu(L1)(H_2O)_2](SO_3CF_3)_2$ **1**
R= CH_3 $[Cu(L2)(H_2O)_2](SO_3CF_3)_2$ **2**

$[Cu(L3)Cl_2]$ **3**

Scheme 1. The structure of copper complexes **1- 3** used in the present study.

Molecular structure and EPR spectra

The single crystal X-ray structure of **2** shown in Figure 1 with selected atom labeling. The complex has been crystallized in a triclinic system with a space group of P-1 (Table 1, Figure 1a and Figure S2) and geometry around copper(II) centre is distorted square pyramidal. This structural geometry revealed by the trigonality index τ of 0.2545 [$\tau = (\beta - \alpha)/60$; β (O1-Cu1-N3) = 173.18° and α (N1-Cu1-N4) = 157.94°; for perfect square pyramidal and trigonal-bipyramidal geometries, τ = 0 and 1 respectively].[18] This square pyramidal coordination

View Article Online
DOI: 10.1039/C7DT01895A

geometry of copper(II) centre is constituted by three nitrogen donors from the ligand and two water molecules. All three nitrogen atoms and one water molecule constitute square plan and remaining axial portion is occupied by a water molecule. The Cu-N_{py} (1.958 Å) of middle pyridine is shorter than other two Cu-N_{Benzim} bonds (Cu-N, 1.995, 2.000 Å). The axial Cu-O2 bond distance (2.247 Å) is slightly longer than the equatorial Cu-O1 bond distance (1.953 Å). The Cu-N bond lengths of **2** are almost similar to those of previously reported $[Cu(L1)(H_2O)_2](NO_3)_2$ (1.98 - 2.034 Å)**.**[19] However, these Cu-N bond distances are shorter than structurally similar **3** (Cu–N_{py},1.970 - 2.069 Å) (Figure 1b). The sum of bond angles N3-Cu1-N4 (79.95°), N3-Cu1-N1 (79.95°), N1-Cu1-O1 (101.37°) and O1-Cu1-N4 (97.55°) is 358.42° and closer to 360° suggesting that N1, N2, N3, and O1 are nearly coplanar in **2**. The N1-Cu-N4 (157.94°) and N3-Cu-O1 (173.18°) bond angles deviate from the 180°, indicating distortion in the square plane.

The square based geometry of **2** is further supported by EPR spectrum (Figure 2). The frozen solution spectra of **2** in methanol/DMF mixture at 70 K was found to be anisotropic and its hyperfine features due to copper have been resolved in the parallel region ($g_{\|} = 2.29$, $g_{\perp} = 2.06$) (Table 2). The EPR spectrum comprises of g values in the order of $g_{\|} > g_{\perp} > 2.0023$ which corresponds to normal EPR spectrum for copper(II) center with square based geometry. Further, the $A_{\|}$ value of 156×10^{-4} cm^{-1} suggested that **2** belongs to square pyramidal geometry ($A_{\|}$ = 154 -162 $\times 10^{-4}$ cm^{-1} for square based geometry[20]). This EPR spectral signature of **2** are similar to that of **1** ($g_{\perp}$, 2.05; $g_{\|}$, 2.29) but the geometrical parameter is higher than **1**($A_{\|}$ 124 $\times 10^{-4}$ cm^{-1}). This reveals stronger geometrical distortion in **1**. However, the $A_{\|}$ value of **2** is closer to that of **3** **(**156.8 $\times 10^{-4}$ cm^{-1}) and $g_{\perp}$ (2.05) and ($g_{\|}$, 2.29) values are similar.

Electronic absorption spectral studies

The complexes **1** and **2** exhibit d-d transitions at 662 (ε, 90 $M^{-1}cm^{-1}$) and 651nm (ε, 84 $M^{-1}cm^{-1}$) respectively along with merged ligand based transitions in the concentration of 1×10^{-2} M in HEPES buffer at pH 7.34 (Table 2, Figure 3). However, π-π* ligand transitions at 309 and 327 nm (ε, 11,480 and 13,020 $M^{-1}cm^{-1}$) for L1 and 313 nm (ε, 10,360 $M^{-1}cm^{-1}$) for L2 are well resolved only at lower concentration (5×10^{-6} M). On coordination of a Cu^{2+} ion with L1 (5×10^{-6} M) in HEPES buffer at pH 7.34, the ligand-based transitions at 309 and 327 nm were disappeared and two new bands were formed at 314 and 356 nm appeared (ε, 19,740 and 13,180

View Article Online
DOI: 10.1039/C7DT01895A

$M^{-1}cm^{-1}$). On other hand, Cu^{2+} ion coordination with L2 shows new bands at 360 nm (ε, 9560 $M^{-1}cm^{-1}$) along with the ligand-based transition at 313 nm (ε, 16,860 $M^{-1}cm^{-1}$). However, the d-d transition is not perceived at this lower concentration. The changes in the d-d bands of **1** and **2** with various amino acids were studied at the concentration of 1×10^{-2} M. The d-d transition of **1** and **2** slightly lowered by addition of various natural amino acids (alanine, arginine, glycine, histidine, leucine, proline, serine, threonine, tryptophan, and tyrosine) (Figure S3e and S3f). However, the d-d band was readily disappeared on the addition of Cys (Figure S3c and S3d). On other hand, the intensity of d-d transition has been decreased by the addition of His to **2** (Figure S5f). At the lower concentration (5×10^{-6} M), the addition of only one equivalent of Cys to **1** and **2** reproduces the absorption pattern of L1 and L2 respectively and all other amino acids exhibited no concomitant changes under identical conditions (Figure S3a, S3b, and Figure S4). These results reveal that the possibility of Cu^{2+} displacement from coordination sphere of **1** and **2** on interaction with Cys (Figure 3). We have reported very similar observation for **3** with Cys under identical conditions.[9] The addition of other biomolecules homocysteine (Hcy) and glutathione (GSH) containing thiol exhibits slight changes in absorption bands of **1** and **2** (Figure S5a, and Figure S5b).

Fluorescence Studies

The ligands L1 and L2 showed strong fluorescence at 406 and 392 nm with the quantum yield of 3.83 % and 11.3 % respectively in HEPES buffer at pH, 7.34 (5×10^{-6} M). Nevertheless, the complexes **1** and **2** are found as non-fluorescent. This is further confirmed by the immediate fluorescence intensity quenching of ligand while adding one equivalent Cu^{2+} ion (Figure S7). This non-fluorescent nature of **1** and **2** raised up by the paramagnetic nature of copper(II) centre, which strongly disturbed the electronic resonance of the ligand and hence lowering in the fluorescence intensity. This is further supported by HOMO-LUMO electron density map obtained by DFT method using B3LYP 6-31G (for C, H, and N)/LANL2DZ (for Cu) basis set in Gaussian 09 program (Table 2, Figure 4, Figure S6).[21] The L1 and L2 show optimized energy, -2.7365×10^4 and -2.9504×10^4 eV respectively, the frontier molecular orbitals HOMO and LUMO are localized across the benzimidazole moiety. However, HOMO and LUMO are localized around benzimidazole moiety and copper centre respectively for **1** and **2**. The ground state energies of complexes are lower (**1**, -6.3894×10^4 eV; **2**, -6.6033×10^4 eV) than that of

View Article Online
DOI: 10.1039/C7DT01895A

ligands. However**,** these HOMO and LUMO of ligand L1 and L2 are different from our previously reported ligand L3, where they are localized on fluorophore unit anthracenyl moiety. The HOMO of **3** localized around the copper centre and LUMO was localized only on terpyridine unit. These results are clearly indicating that electronic resonance of benzimidazole moiety is strongly disrupted by Cu^{2+} centre via internal charge transfer and hence quenching of fluorescence intensity and change in absorption spectral pattern (cf. above).

The treatment of **1** and **2** with various amino acids (Figure 5 and 6) show no enhancement in the fluorescence intensity. However, the interaction of Cys (5×10^{-5} M) with **1** enhances the fluorescence intensity almost 1.3 and 28 times higher than the original intensity of L1 and **1** respectively with a quantum yield of 14.7 % in aqueous solution. This increase in fluorescence intensity has been saturated at 15 equivalents of Cys and no enhancement on further more addition **(**Figure 7a). A huge fluorescence enhancement was observed for **2** with Cys and this enhancement 143 times higher than that of **2** with a quantum yield of 23%. The increase in intensity has been saturated with 13 equivalents of Cys and subsequent equivalents have shown no further enhancement (Figure 7b).Thus, almost a similar enhancement in fluorescence intensity has been noticed for **1** and **2** with the similar probing mechanism. Further, these fluorescence responses of **1** and **2** with Cys are similar to that of our previously reported complex **3** with Cys and showed 'turn-on' mechanism with the quantum yield of 6% in 5×10^{-6} M at pH 7.34.[9] The fluorescence intensity was raised by the addition of His to **1** and **2** with a quantum yield of 5 and 11.3 % respectively. However, the increase in the emission intensity is 50% lower than that of Cys and saturated with 15 and 13 equivalents of His for **1** and **2** respectively (Figure S8b and S9b). On other hand, Hcy and *N*-acetyl-L-cysteine (NAC) with **1** and **2** were shown significantly lower enhanced of fluorescence intensity than Cys. However, the fluorescent intensity enhancement by GSH with **1** and **2** is comparatively negligible (Figure S10).

The fluorescence titration of **1** and **2** with Cys and His have been followed the Hildebrand-Benesi equation, $I_0/I\text{-}I_0 = b/(a - b)\ \{1/(K[M]) + 1\}$ where, I_0 and I are intensities in the absence and presence of analyte respectively, $[M]$ is the concentration of analyte, a and b are intercept and slope of the plot respectively. The linear plot was obtained by fitting $(I_0/I\text{-}I_0)$ vs $1/[M]$.[8d] Upon addition of small aliquots of Cys to **1** and **2** raised the fluorescence intensity gradually and they were found to be linear (Figure 8). The binding constant values were

View Article Online
DOI: 10.1039/C7DT01895A

calculated as 5.403×10^4 and 1.307×10^4 M^{-1} for **1** and **2** respectively. The limit of detection was calculated by employing the formula [3 × (Standard deviation/slope)] from the linear plot and **1** and **2**, shows 2.9×10^{-8} M and 3.32×10^{-8} M respectively. These binding constant values are slightly lower than that of **3 (**7.7×10^4 M^{-1}) but the limit of detection values are almost similar to **3 (**1.9×10^{-8} M). The fluorescence studies revealed that **1** and **2** are highly selective towards Cys and it can detect Cys even at lower concentration level. The competitive experiments of one equivalent of Cys with 20 equivalents of other natural amino acids show that fluorescence intensity readily raised only by Cys. Thus, the fluorescence intensity enhancement of **1** and **2** with Cys (Figure S12) is not affected by 20 equivalents of other natural amino acids. On other hand, the binding constant values calculated for His with **1** and **2** as 1.4031×10^5 and 7.554×10^4 M^{-1} respectively are almost similar to that of Cys. However the limit of detection values 8.03×10^{-7} M and 2.32×10^{-7} M for **1** and **2** respectively are lower than the values of Cys (Figure S11 and Figure S13).

Redox properties

The redox behavior of **1** and **2** has been investigated by cyclic voltammetry (CV) using a three-electrode cell configuration in HEPES buffer solution at pH, 7.34 and NaCl was used as supporting electrolyte. A platinum sphere, a platinum wire, and Ag/Ag^+ were used as working, auxiliary and reference electrodes respectively. The measured redox potential was converted into NHE (normal hydrogen electrode) by adding +0.205 V. The irreversible Cu(II)/Cu(I) redox couples at $E_{1/2}$, 0.014 and 0.233 V vs NHE have been observed for **1** and **2** respectively. Interestingly, this Cu(II)/Cu(I) redox couples were readily disappeared on the addition of four equivalents Cys and new cathodic peak potential has been formed around 0.245 - 0.316 V vs NHE (Table 2, Figure 9). The cathodic peak potential is identical to that of observed for in situ generated Cu^{2+}-Cys species. This is possibly due to the reduction of Cu(II) to Cu(I) by Cys and this redox process is presumed to involve a significant geometrical reorganization from the internal changes in bond lengths and angles of the complex.[6k, 22] The interaction of His with **1** and **2** shows a formation of new redox potentials at 0.1605 and 0.077 V vs NHE for **1** and **2** respectively. This indicates that the coordination of His with the complexes rather than reduction of copper(II) centre and followed release as noticed Cys (Table 2, Figure S14).

View Article Online
DOI: 10.1039/C7DT01895A

The solution of **1** and **2** with one equivalent of Cys were analyzed by ESI-MS and showed the molecular ion peak at 311.98 and 340.03 corresponds to L1 and L2 respectively (Figure S15). The FT-IR analysis exhibits stretching frequencies ($\bar{\upsilon}$) at 3034, 1581, 1485 for **1** and 1406 cm^{-} and 3019, 1584, 1484 and 1405 cm^{-1} for **2,** which are matched with stretching frequencies of in situ generated Cu^{2+}-Cys species (Figure S17).[23] The ESI-MS and FT-IR studies reveal that presumably copper displacement from coordination sphere and release of the free ligand as noticed by the electronic spectra and electrochemistry. Thus, the enhancement in fluorescence intensity of **1** and **2** with Cys presumably proceeds via two consecutive steps, firstly the copper(II) centre is reduced to copper(I) by Cys as expected. Once reduced, the copper(I) ion is apparently released from coordination sphere, owing to its preference for tetrahedral coordination geometry [6k, 21] but the rigid pyridine-bis-benzimidazole ligand system is unable to adopt this preference (Scheme 2). Then the electron density of ligand is possibly regenerated around the fluorophore for the emission. Further, the Cu(II)/Cu(I) redox potential of **1** and **2** are much lower than a reported redox barrier for adopting tetrahedral geometry as known in the blue copper proteins ($E_{1/2}$, 0.276 - 0.307 V).[24] On other hand , the amino acid His coordinates with **1** and **2** and produces 'turn-on' fluorescence enhancement by transferring the electron density towards benzimidazole units from copper centre. This is further supported by DFT studies, revealing that HOMO and HOMO-1 orbitals are localized on the histidine units and LUMO and LUMO +1 are localized on benzimidazole units (Figure 10). This is consistent with ESI-MS spectra of **1** and **2** with His, shows the species *m/z*, 684.10 and 684.33 corresponding to $[(L1)Cu(His)_2]^+$ and $[(L2)Cu(His)(MeOH)_4]^+$ respectively (Figure S16).

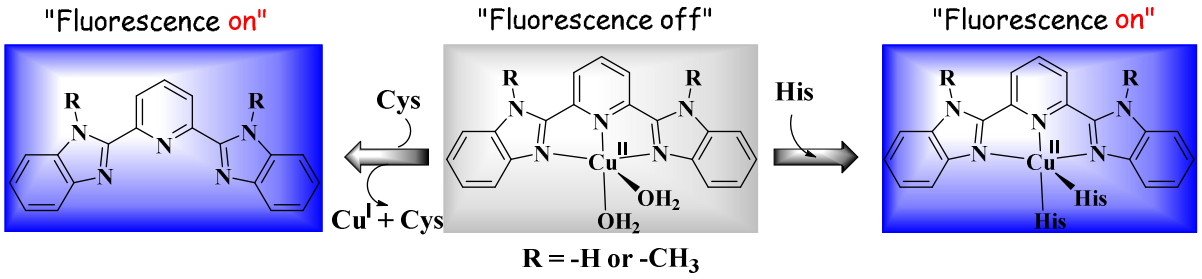

Scheme 2. Proposed mechanism for Cys and His detection by **1** and **2**.

Conclusions

View Article Online
DOI: 10.1039/C7DT01895A

The copper(II) complexes of 2,6-bis(1H-benzo[d]imidazol-2-yl)pyridine ligands L1 and L2 have been synthesized as a probe for Cys. The molecular structure of probe **2** adopts square pyramidal geometry around copper(II) centre and it is further supported by EPR spectral data. The probes showed a selective and efficient "turn-on" fluorescence behavior towards Cys over other natural amino acids at pH, 7.34 with the excellent binding constants values with the limit of detection around 10^{-8} M at pH, 7.34. The redox, ESI-Mass and IR studies revealed that the probe showed bright visible-light emission on reacts with Cys by reduction of copper(II) centre to copper(I) and subsequent displacement of copper. Because, the rigid pyridine-bis-benzimidazole ligand systems unable to adopt preferable tetrahedral coordination geometry of copper(I) which leads to collapsing of coordination sphere, subsequently original fluorescence intensity of ligand is turned-on. On other hand, a relatively small fluorescence enhancement by probes with histidine unit via the coordination of His rather than the displacement of copper, which produces through releasing electron density to the benzimidazole units from the copper centre.

Experimental Section

Materials: Unless otherwise indicated, common reagents or materials were obtained from the commercial source and used without further purification. All the solvents were used after appropriate distillation or purification. The chemicals 2,6-pyridine-dicarboxylic acid, 1,2-diaminobenzene, Polyphosphoric acid, methyl Iodide, ammonium hydroxide, potassium hydroxide, copper triflate, amino acids like L-Alanine, L-Cysteine, L-Glycine, L-Histidine, L-Leucine, L-Proline, L-Serine, L-Threonine, L-Tryptophan were purchased from Sigma-Aldrich and used as such without further purification.

Physical Measurements: All reactions were carried out under an atmosphere of dry nitrogen. Glassware was oven dried prior to use. Unless otherwise indicated, common reagents or materials were obtained from the commercial source and used without further purification. All the solvents were used after appropriate distillation or purification. NMR spectra were recorded at 300 MHz on a Bruker spectrometer. Chemicals shifts values and coupling constants are given in ppm and Hz respectively. ESI-MS spectra were measured on a Thermo LC-MS instrument. Absorption spectra were carried out using Agilent diode array 8453 spectrometer at 298 K and Emission spectra were measured on Agilent Cary Eclipse Spectrofluorometric at 298 K.

View Article Online
DOI: 10.1039/C7DT01895A

Electrochemical data were recorded in Biologic SP-150 Electrochemical workstation using saturated Ag/Ag^+ and Pt as a reference electrode and working electrodes respectively. The 0.1 M NaCl is used as supporting electrolyte. The electrodes are calibrated by $K_4[Fe(CN)_6]$ prior to measurements. IR spectra were taken in Shimadzu FT-IR instrument. Electron paramagnetic resonance (EPR) measurements were recorded using Bruker EMX Plus EPR Spectrometer.

X-ray Structure Determination: Single crystal **2** of suitable size was picked from the mother liquor, coated with paraffin oil and mounted on a fiber loop for X-ray diffraction data collection on Agilent Supernova system (Cu-Kα radiation) equipped with Titan CCD detector. Data processing, including face based absorption correction, was carried out using CrysAlisPro software suites. The structure was solved by the direct method using Shelxs and refined using Shelxl.[25] All the non-hydrogen atoms were refined anisotropically, whereas the hydrogen atoms were added at the riding positions and refined isotropically. CCDC-1551263 contain the supplementary crystallographic data for this paper. This data can be obtained free of charge from The Cambridge Crystallographic Data Centre via ww.ccdc.cam.ac.uk/data request/cif.

DFT Methods: The geometry optimizations were performed by using density functional theory (DFT) methods. For the metal ion involving systems using LANL2DZ basis sets with the Becke3–Lee–Yang–Parr hybrid functional (B3LYP) and the 6−311G (d) basis sets used for elements other than metals. All DFT calculations were carried out by using the Gaussian 09 program package.[26]

Synthesis of 2,6-bis(1H-benzo[d]imidazol-2-yl)pyridine (L1)

This ligand was synthesized and characterized by a previously reported method.[11] ^{1}H NMR (d6-DMSO, 300 MHz): δ 8.31 (d, J = 7.8 Hz, 2H), 7.99 (t, J = 7.8 Hz, 1H), 7.73 (d, J = 7.3 Hz, 2H), 7.60 (d, J = 7.1 Hz, 2H), 7.25 (t, J = 7.8 Hz, 4H) ppm. ESI-MS (*m/z*): [$C_{19}H_{14}N_5^+$], 312.84.

Synthesis of 2,6-bis(1-methyl-1H-benzo[d]imidazol-2-yl)pyridine (L2)

The ligand L2 was also synthesized and characterized as described previously.[11] ^{1}H NMR (d6-DMSO, 300 MHz): δ 8.30 (d, J = 9.6 Hz, 2H), 7.98 (t, J = 8.7 Hz, 1H), 7.69 (d, J = 7.5 Hz,

View Article Online
DOI: 10.1039/C7DT01895A

2H), 7.41 (d, *J* = 7.8 Hz, 2H), 7.24 (dt, *J* = 13.3, 6.7 Hz, 4H), 4.18 (s, 6H) ppm. ESI-MS (m/z): $[C_{21}H_{18}N_5^+]$, 340.44.

Synthesis of $[Cu(L1)(H_2O)_2](SO_3CF_3)_2$ 1

The ligand L1 (0.155 g, 0.5 mmol) was dissolved in 10 mL of hot methanol and $Cu(SO_3CF_3)_2$ (0.5 mmol) in 5 mL of methanol was added dropwise and stirred for 30 minutes at 55°C. A green coloured product was filtered off and washed with cold methanol and diethyl ether to remove excess ligand. Then it was dried under vacuum. Yield: 0.171 g (91.4%). HR-ESI-MS (*m/z*): [((L1)Cu(H_2O))/2]2MeOH, 226.0285; [(L1)Cu]+2H^+, 375.0383 and [(L1)Cu($H_2O)_2$]+H^+, 411.0143.

Synthesis of $[Cu(L2)(H_2O)_2](SO_3CF_3)_2$ **2**

The complex **2** was synthesized by using above procedure. The ligand L2 was used instead of ligand L1. Yield: 0.083 g (72%). HR-ESI-MS: (*m/z*): $[((L2)Cu)/2]^+$, 201.0388; $[((L2)Cu\ (H_2O)_4)/2 + 3H]^+$; 240.0460, $[(L2)Cu(H_2O)_2]^+$, 438.0898.

Acknowledgements

We acknowledge Science and Engineering Research Board (SERB), New Delhi, Board of Research in Nuclear Sciences (BRNS), Mumbai and Department of Biotechnology (DBT), New Delhi for funding. DM thanks to University Grants Commission (UGC), New Delhi for fellowship.

References

1. R. K. Pathak, K. Tabbasum, A. Rai, D. Panda and C. P. Rao, *The Analyst*, 2012, **137**, 4069-4075.
2. (a) M. Zhang, M. Yu, F. Li, M. Zhu, M. Li, Y. Gao, L. Li, Z. Liu, J. Zhang, D. Zhang, T. Yi and C. Huang, *J. Am. Chem. Soc.*, 2007, **129**, 10322-10323; (b) C. Yin, F. Huo, J. Zhang, R. Martinez-Manez, Y. Yang, H. Lv and S. Li, *Chem. Soc. Rev.*, 2013, **42**, 6032-6059; (c) X. Yuan, Y. Tay, X. Dou, Z. Luo, D. T. Leong and J. Xie, *Anal. Chem.*, 2013, **85**, 1913-1919.
3. (a) N. Jacob, E. Bruckert, P. Giral, M. J. Foglietti and G. Turpin, *Atherosclerosis*, 1999, **146**, 53-59; (b) S. Shahrokhian, *Anal. Chem.*, 2001, **73**, 5972-5978; (c) S. P. Lutgens, K. B. Cleutjens, M. J. Daemen and S. Heeneman, *FASEB J.*, 2007, **21**, 3029-3041; (d) L. Urbanelli, C. Emiliani, C. Massini, E. Persichetti, A. Orlacchio, G. Pelicci, S. Sorbi, A. Hasilik, G. Bernardi and A. Orlacchio, *Neurobiol. Aging*, 2008, **29**, 12-22; (e) T. T.

View Article Online
DOI: 10.1039/C7DT01895A

Rohn, *Apoptosis*, 2010, **15**, 1403-1409; (f) E. Weerapana, C. Wang, G. M. Simon, F. Richter, S. Khare, M. B. D. Dillon, D. A. Bachovchin, K. Mowen, D. Baker and B. F. Cravatt, *Nature*, 2010, **468**, 790-795; (g) X. W. Cheng, G. P. Shi, M. Kuzuya, T. Sasaki, K. Okumura and T. Murohara, *Circulation*, 2012, **125**, 1551-1562; (h) E. Lee, J. E. Eom, H. L. Kim, K. H. Baek, K. Y. Jun, H. J. Kim, M. Lee, I. Mook-Jung and Y. Kwon, *Biochim. Biophys. Acta*, 2013, **1831**, 709-718; (i) S. Hasanbasic, A. Jahic, E. Karahmet, A. Sejranic and a. Prnjavorac, *Mater. Sociomed.*, 2016, **28**, 235.

4. (a) J. A. Joyce and D. Hanahan, *Cell Cycle*, 2004, **3**, 1516-1519; (b) V. Turk, J. Kos and B. Turk, *Cancer Cell*, 2004, **5**, 409-410; (c) M. M. Mohamed and B. F. Sloane, *Nature reviews. Cancer*, 2006, **6**, 764-775; (d) L. Klein, M. Hinterberger, G. Wirnsberger and B. Kyewski, *Nat. Rev. Immunol.*, 2009, **9**, 833-844; (e) S. P. Fricker, *Metallomics*, 2010, **2**, 366-377; (f) V. Turk, V. Stoka, O. Vasiljeva, M. Renko, T. Sun, B. Turk and D. Turk, *Biochim. Biophys. Acta*, 2012, **1824**, 68-88; (g) G. J. Tan, Z. K. Peng, J. P. Lu and F. Q. Tang, *World. J. Biol. Chem.*, 2013, **4**, 91-101.
5. (a) A. Ito, S. Ishizaka and N. Kitamura, *Phys. Chem. Chem. Phys.*, 2010, **12**, 6641-6649; (b) L.-Y. Niu, Y.-S. Guan, Y.-Z. Chen, L.-Z. Wu, C.-H. Tung and Q.-Z. Yang, *Chem. Commun.*, 2013, **49**, 1294-1296; (c) T. Minami, N. A. Esipenko, B. Zhang, L. Isaacs and P. Anzenbacher, Jr., *Chem Commun (Camb)*, 2014, **50**, 61-63; (d) Y. Zhou and J. Yoon, *Chem. Soc. Rev.*, 2012, **41**, 52-67.
6. (a) Y. Kanaoka, *Angew. Chem. Int. Ed*, 1977, **16**, 137-147; (b) A. P. de Silva and K. R. A. S. Sandanayake, *Angew. Chem. Int. Ed*, 1990, **29**, 1173-1175; (c) Y. Kubo, S. y. Maeda, S. Tokita and M. Kubo, *Nature*, 1996, **382**, 522-524; (d) T. Mizutani, K. Wada and S. Kitagawa, *J. Am. Chem. Soc.*, 1999, **121**, 11425-11431; (e) P. Anzenbacher, A. C. Try, H. Miyaji, K. Jursíková, V. M. Lynch, M. Marquez and J. L. Sessler, *J. Am. Chem. Soc.*, 2000, **122**, 10268-10272; (f) H. Miyaji, W. Sato and J. L. Sessler, *Angew. Chem. Int. Ed.*, 2000, **39**, 1777-1780; (g) H. Aït-Haddou, S. L. Wiskur, V. M. Lynch and E. V. Anslyn, *J. Am. Chem. Soc.*, 2001, **123**, 11296-11297; (h) H. Imai, K. Misawa, H. Munakata and Y. Uemori, *Chem. Lett.*, 2001, **30**, 688-689; (i) H. Miyaji and J. L. Sessler, *Angew. Chem. Int. Ed.*, 2001, **40**, 154-157; (j) E. K. Feuster and T. E. Glass, *J. Am. Chem. Soc.*, 2003, **125**, 16174-16175; (k) O. Rusin, N. N. St. Luce, R. A. Agbaria, J. O. Escobedo, S. Jiang, I. M. Warner, F. B. Dawan, K. Lian and R. M. Strongin, *J. Am. Chem. Soc.*, 2004, **126**, 438-439; (l) W.-L. Wong, K.-H. Huang, P.-F. Teng, C.-S. Lee and H.-L. Kwong, *Chem. Commun.*, 2004, 384-385; (m) S.-H. Li, C.-W. Yu and J.-G. Xu, *Chem. Commun.*, 2005, 450-452; (n) S. Xu, K. Chen and H. Tian, *J. Mater. Chem.*, 2005, **15**, 2676-2680; (o) H. Chen, Q. Zhao, Y. Wu, F. Li, H. Yang, T. Yi and C. Huang, *Inorg. Chem.*, 2007, **46**, 11075-11081; (p) X. Chen, Y. Zhou, X. Peng and J. Yoon, *Chem. Soc. Rev.*, 2010, **39**, 2120-2135.
7. (a) J. Gonzalez, J. M. Llinares, R. Belda, J. Pitarch, C. Soriano, R. Tejero, B. Verdejo and E. Garcia-Espana, *Org. Bio. Chem.*, 2010, **8**, 2367-2376; (b) A. Y. Cho and K. Choi, *Chem. Lett.*, 2012, **41**, 1611-1612; (c) L. Y. Niu, Y. S. Guan, Y. Z. Chen, L. Z. Wu, C. H. Tung and Q. Z. Yang, *J. Am. Chem. Soc.*, 2012, **134**, 18928-18931; (d) L. Yuan, W. Lin, S. Zhao, W. Gao, B. Chen, L. He and S. Zhu, *J. Am. Chem. Soc.*, 2012, **134**, 13510-13523; (e) L.-Y. Niu, H.-R. Zheng, Y.-Z. Chen, L.-Z. Wu, C.-H. Tung and Q.-Z. Yang, *The Analyst*, 2014, **139**, 1389-1395; (f) F. Wang, Z. Guo, X. Li, X. Li and C. Zhao, *Chemistry*, 2014, **20**, 11471-11478; (g) J. Yin, Y. Kwon, D. Kim, D. Lee, G. Kim, Y. Hu, J. H. Ryu and J. Yoon, *J. Am. Chem. Soc.*, 2014, **136**, 5351-5358; (h) C. Ge, H. Wang, B.

View Article Online
DOI: 10.1039/C7DT01895A

Zhang, J. Yao, X. Li, W. Feng, P. Zhou, Y. Wang and J. Fang, *Chem. Commun.*, 2015, **51**, 14913-14916; (i) Y. Hu, C. H. Heo, G. Kim, E. J. Jun, J. Yin, H. M. Kim and J. Yoon, *Anal. Chem.*, 2015, **87**, 3308-3313; (j) M.-Y. Jia, L.-Y. Niu, Y. Zhang, Q.-Z. Yang, C.-H. Tung, Y.-F. Guan and L. Feng, *ACS Appl. Mater. Interfaces*, 2015, **7**, 5907-5914; (k) T. Ma, H. Ding, H. Xu, Y. Lv, H. Liu, H. Wang and Z. Tian, *The Analyst*, 2015, **140**, 322-329; (l) Q. Miao, Q. Li, Q. Yuan, L. Li, Z. Hai, S. Liu and G. Liang, *Anal. Chem.*, 2015, **87**, 3460-3466; (m) F. Wang, L. Zhou, C. Zhao, R. Wang, Q. Fei, S. Luo, Z. Guo, H. Tian and W.-H. Zhu, *Chem. Sci.*, 2015, **6**, 2584-2589; (n) J. Zhang, J. Wang, J. Liu, L. Ning, X. Zhu, B. Yu, X. Liu, X. Yao and H. Zhang, *Anal. Chem.*, 2015, **87**, 4856-4863; (o) D. Zhang, Z. Yang, H. Li, Z. Pei, S. Sun and Y. Xu, *Chem. Commun.*, 2016, **52**, 749-752; (p) X. Chen, Y. Zhou, X. Peng and J. Yoon, *Chem. Soc. Rev.*, 2010, **39**, 2120-2135; (q) Y. Zhou and J. Yoon, *Chem. Soc. Rev.*, 2012, **41**, 52-67; (r) H. S. Jung, X. Chen, J. S. Kim and J. Yoon, *Chem. Soc. Rev.*, 2013, **42**, 6019-6031; (s) L. Y. Niu, Y. Z. Chen, H. R. Zheng, L. Z. Wu, C. H. Tung and Q. Z. Yang, *Chem. Soc. Rev.*, 2015, **44**, 6143-6160.

8. (a) Y. Fu, H. Li, W. Hu and D. Zhu, *Chem. Commun.*, 2005, 3189-3191; (b) W. Hao, A. McBride, S. McBride, J. P. Gao and Z. Y. Wang, *J. Mater. Chem.*, 2011, **21**, 1040-1048; (c) H. S. Jung, J. H. Han, Y. Habata, C. Kang and J. S. Kim, *Chem. Commun.*, 2011, **47**, 5142-5144; (d) Z. Huang, J. Du, J. Zhang, X. Q. Yu and L. Pu, *Chem. Commun.*, 2012, **48**, 3412-3414; (e) Y. G. Shi, J. H. Yao, Y. L. Duan, Q. L. Mi, J. H. Chen, Q. Q. Xu, G. Z. Gou, Y. Zhou and J. F. Zhang, *Bioorg. Med. Chem. Lett.*, 2013, **23**, 2538-2542; (f) U. R. G, H. Agarwalla, N. Taye, S. Ghorai, S. Chattopadhyay and A. Das, *Chem. Commun.*, 2014, **50**, 9899-9902; (g) C.-C. Zhao, Y. Chen, H.-Y. Zhang, B.-J. Zhou, X.-J. Lv and W.-F. Fu, *J. Photochem. Photobiol., A*, 2014, **282**, 41-46; (h) K.-S. Lee, J. Park, H.-J. Park, Y. K. Chung, S. B. Park, H.-J. Kim, I.-S. Shin and J.-I. Hong, *Sens. Actuators B Chem.*, 2016, **237**, 256-261.
9. D. Maheshwaran, T. Nagendraraj, P. Manimaran, B. Ashokkumar, M. Kumar and R. Mayilmurugan, *Eur. J. Inorg. Chem.*, 2017, **2017**, 1007-1016.
10. M. H. Lim, B. A. Wong, W. H. Pitcock, D. Mokshagundam, M.-H. Baik and S. J. Lippard, *J. Am. Chem. Soc.*, 2006, **128**, 14364-14373.
11. I. Mathew and W. Sun, *Dalton Trans*, 2010, **39**, 5885-5898.
12. (a) F. Chavez and A. D. Sherry, *J.Org. Chem.*, 1989, **54**, 2990-2992; (b) E. R. Nelson, M. Maienthal, L. A. Lane and A. A. Benderly, *J. Am. Chem. Soc.*, 1957, **79**, 3467-3469; (c) A. Ojida, Y. Mito-oka, M.-a. Inoue and I. Hamachi, *J. Am. Chem. Soc.*, 2002, **124**, 6256-6258; (d) S. S. Alguindigue, M. A. Khan and M. T. Ashby, *Inorg. Chim. Acta*, 2000, **310**, 156-162.
13. (a) G. Roelfes, M. E. Branum, L. Wang, L. Que and B. L. Feringa, *J. Am. Chem. Soc.*, 2000, **122**, 11517-11518; (b) J. E. Richman and T. J. Atkins, *J. Am. Chem. Soc.*, 1974, **96**, 2268-2270.
14. (a) H. Su, C. Wu, J. Zhu, T. Miao, D. Wang, C. Xia, X. Zhao, Q. Gong, B. Song and H. Ai, *Dalton Trans.*, 2012, **41**, 14480-14483; (b) L. A. Carpino, *Acc. Chem. Res.*, 1987, **20**, 401-407.
15. (a) E. Rodríguez, R. Simoes, A. Roig, E. Molins, N. Nedelko, A. Ślawska-Waniewska, S. Aime, C. Arús, M. Cabañas, C. Sanfeliu, S. Cerdán and M. García-Martín, *Magn. Reson. Mater. Phys., Biol. Med.*, 2007, **20**, 27-37; (b) L.-L. Zhou, H. Sun, X.-H. Zhang and S.-K. Wu, *Spectrochim. Acta Part A*, 2005, **61**, 61-65.

View Article Online
DOI: 10.1039/C7DT01895A

16. H. E. Gottlieb, V. Kotlyar and A. Nudelman, *J. Org. Chem.*, 1997, **62**, 7512-7515.
17. A. Klapars, X. Huang and S. L. Buchwald, *J. Am. Chem. Soc.*, 2002, **124**, 7421-7428.
18. A. W. Addison, T. N. Rao, J. Reedijk, J. van Rijn and G. C. Verschoor, *J. Chem. Soc., Dalton Trans.*, 1984, 1349-1356.
19. (a) S. Dey, S. Sarkar, H. Paul, E. Zangrando and P. Chattopadhyay, *Polyhedron*, 2010, **29**, 1583-1587; (b) J. García-Lozano, J. Server-Carrió, E. Coret, J.-V. Folgado, E. Escrivà and R. Ballesteros, *Inorg. Chim. Acta*, 1996, **245**, 75-79.
20. B. J. Hathaway and A. A. G. Tomlinson, *Coord. Chem. Rev.*, 1970, **5**, 1-43.
21. Y. Ke, J. Zhao, U. H. Verkerk, A. C. Hopkinson and K. W. M. Siu, *J. Phys. Chem. B*, 2007, **111**, 14318-14328.
22. (a) D. B. Rorabacher, *Chem. Rev.*, 2004, **104**, 651-697; (b) E. I. Solomon, D. E. Heppner, E. M. Johnston, J. W. Ginsbach, J. Cirera, M. Qayyum, M. T. Kieber-Emmons, C. H. Kjaergaard, R. G. Hadt and L. Tian, *Chem. Rev.*, 2014, **114**, 3659-3853; (c) S. Kim, M. A. Minier, A. Loas, S. Becker, F. Wang and S. J. Lippard, *J. Am. Chem. Soc.*, 2016, **138**, 1804-1807.
23. (a) A. Rigo, A. Corazza, M. L. di Paolo, M. Rossetto, R. Ugolini and M. Scarpa, *J. Inorg. Biochem.*, 2004, **98**, 1495-1501; (b) K. M. Dokken, J. G. Parsons, J. McClure and J. L. Gardea-Torresdey, *Inorg. Chim. Acta*, 2009, **362**, 395-401.
24. G. Battistuzzi, M. Borsari, L. Loschi, F. Righi and M. Sola, *J. Am. Chem. Soc.*, 1999, **121**, 501-506.
25. (a) R. Blessing, *Acta Crystallogr. Sect. A*, 1995, **51**, 33-38; (b) L. Palatinus and G. Chapuis, *J. Appl. Crystallogr.*, 2007, **40**, 786-790; (c) O. V. Dolomanov, L. J. Bourhis, R. J. Gildea, J. A. K. Howard and H. Puschmann, *J. Appl. Crystallogr.*, 2009, **42**, 339-341.
26. M. J. Frisch, G. W. Trucks, H. B. Schlegel, G. E. Scuseria, M. A. Robb, J. R. Cheeseman, G. Scalmani, V. Barone, B. Mennucci, G. A. Petersson, H. Nakatsuji, M. Caricato, X. Li, H. P. Hratchian, A. F. Izmaylov, J. Bloino, G. Zheng, J. L. Sonnenberg, M. Hada, M. Ehara, K. Toyota, R. Fukuda, J. Hasegawa, M. Ishida, T. Nakajima, Y. Honda, O. Kitao, H. Nakai, T. Vreven, J. A. Montgomery Jr., J. E. Peralta, F. Ogliaro, M. J. Bearpark, J. Heyd, E. N. Brothers, K. N. Kudin, V. N. Staroverov, R. Kobayashi, J. Normand, K. Raghavachari, A. P. Rendell, J. C. Burant, S. S. Iyengar, J. Tomasi, M. Cossi, N. Rega, N. J. Millam, M. Klene, J. E. Knox, J. B. Cross, V. Bakken, C. Adamo, J. Jaramillo, R. Gomperts, R. E. Stratmann, O. Yazyev, A. J. Austin, R. Cammi, C. Pomelli, J. W. Ochterski, R. L. Martin, K. Morokuma, V. G. Zakrzewski, G. A. Voth, P. Salvador, J. J. Dannenberg, S. Dapprich, A. D. Daniels, Ö. Farkas, J. B. Foresman, J. V. Ortiz, J. Cioslowski and D. J. Fox, *Gaussian 09*, 2009.

View Article Online
DOI: 10.1039/C7DT01895A

Figures and Tables

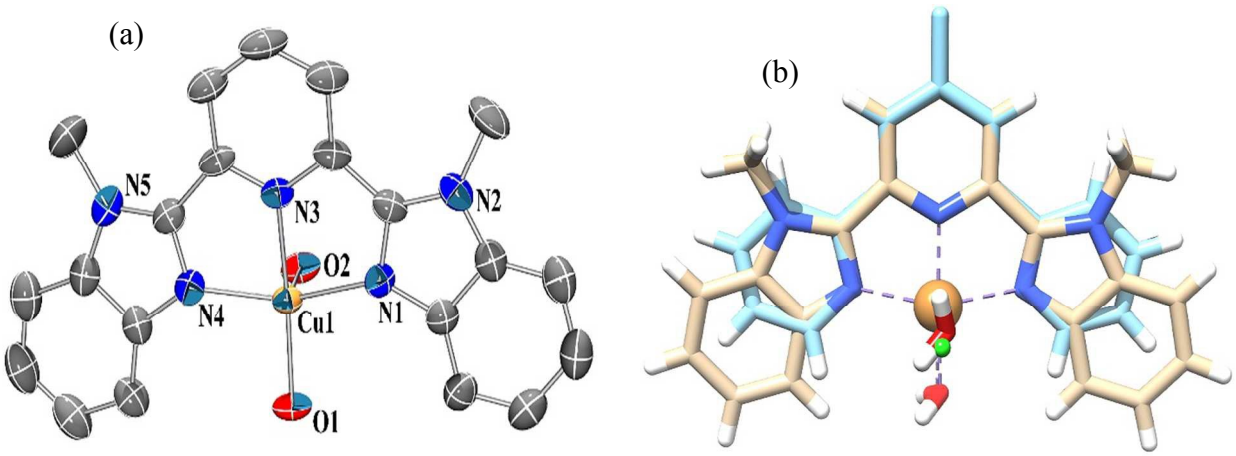

Figure 1. Single crystal X-ray crystal structure of **2** (a) and its overlay with **3** (b). Thermal ellipsoids are shown at the 50% probability level. Hydrogen atoms and $SO_3CF_3^-$ are omitted for clarity.

View Article Online
DOI: 10.1039/C7DT01895A

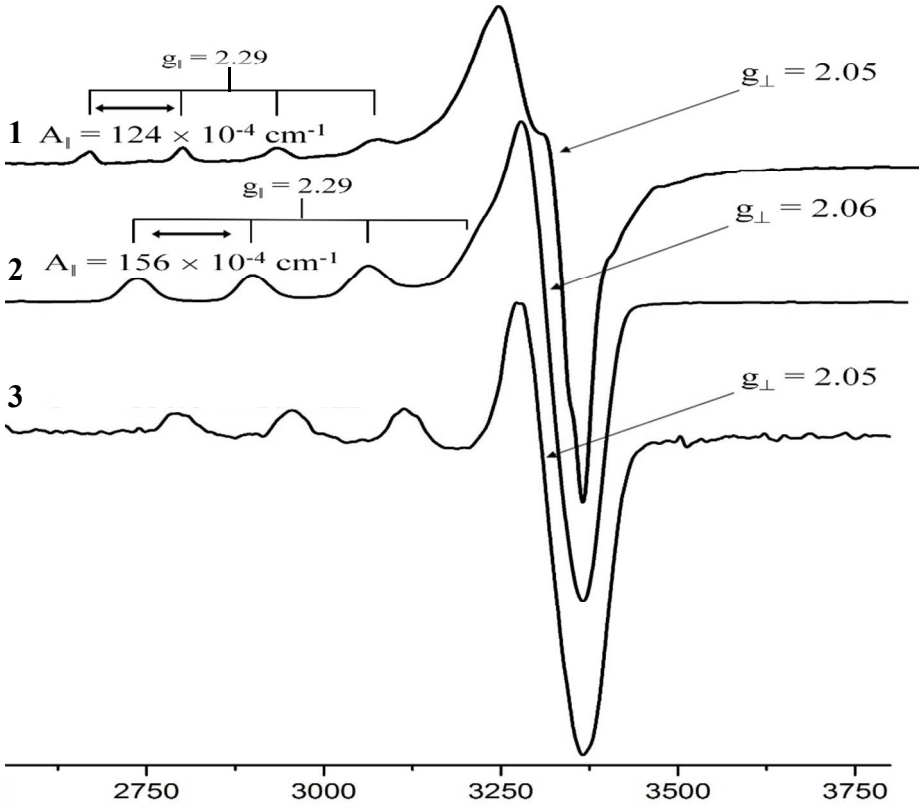

Figure 2. X-band EPR spectra of **1-3** in methanol/DMF mixture at 70 K.

View Article Online
DOI: 10.1039/C7DT01895A

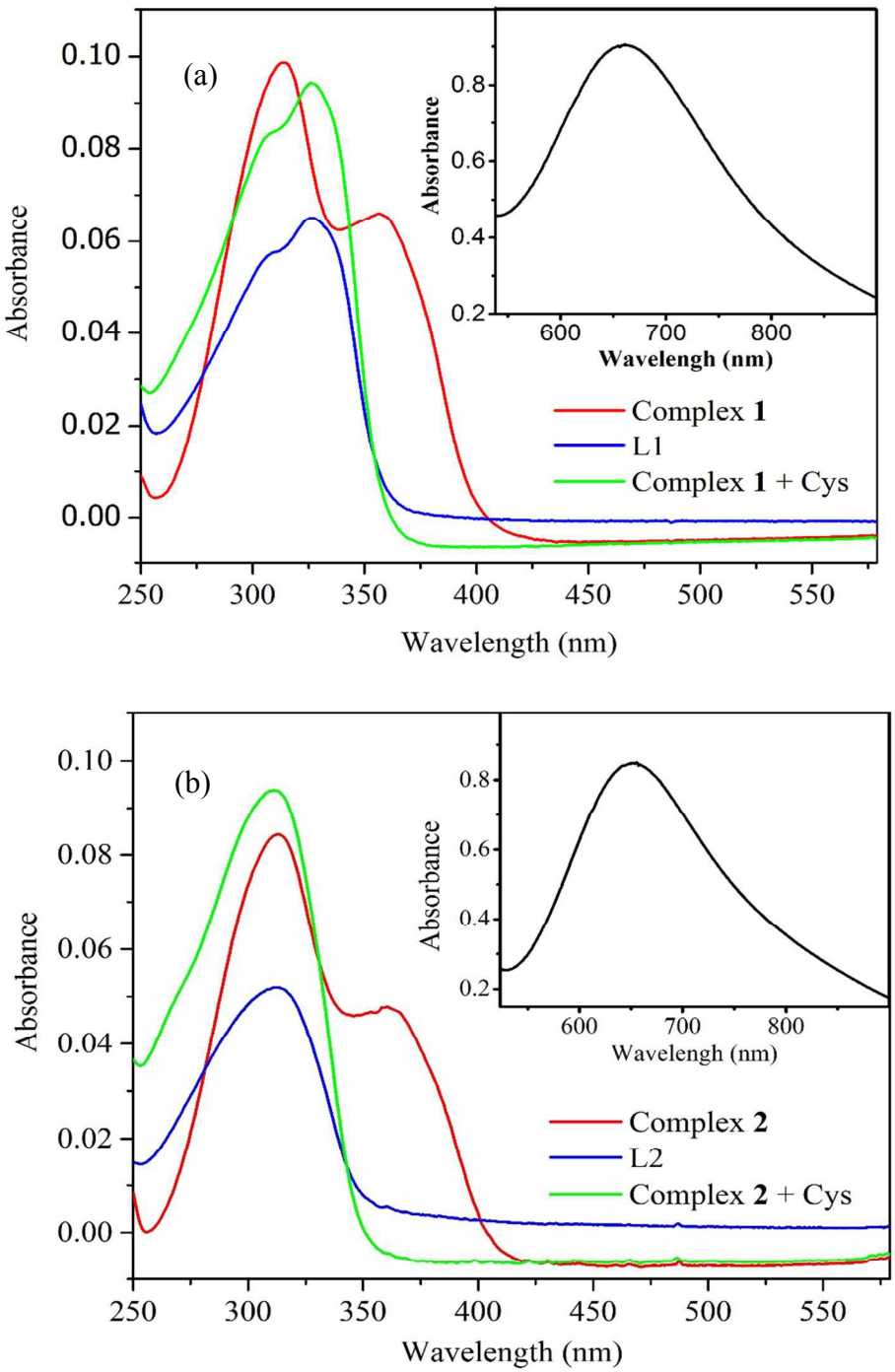

Figure 3. UV-Visible spectra of L1, **1** and **1** + Cys (a) and L1, **2** and **2** + Cys (b), pH 7.34 at 25°C in HEPES buffer (5×10^{-6} M). Insets: d-d transitions of corresponding complexes at 1×10^{-2} M.

View Article Online
DOI: 10.1039/C7DT01895A

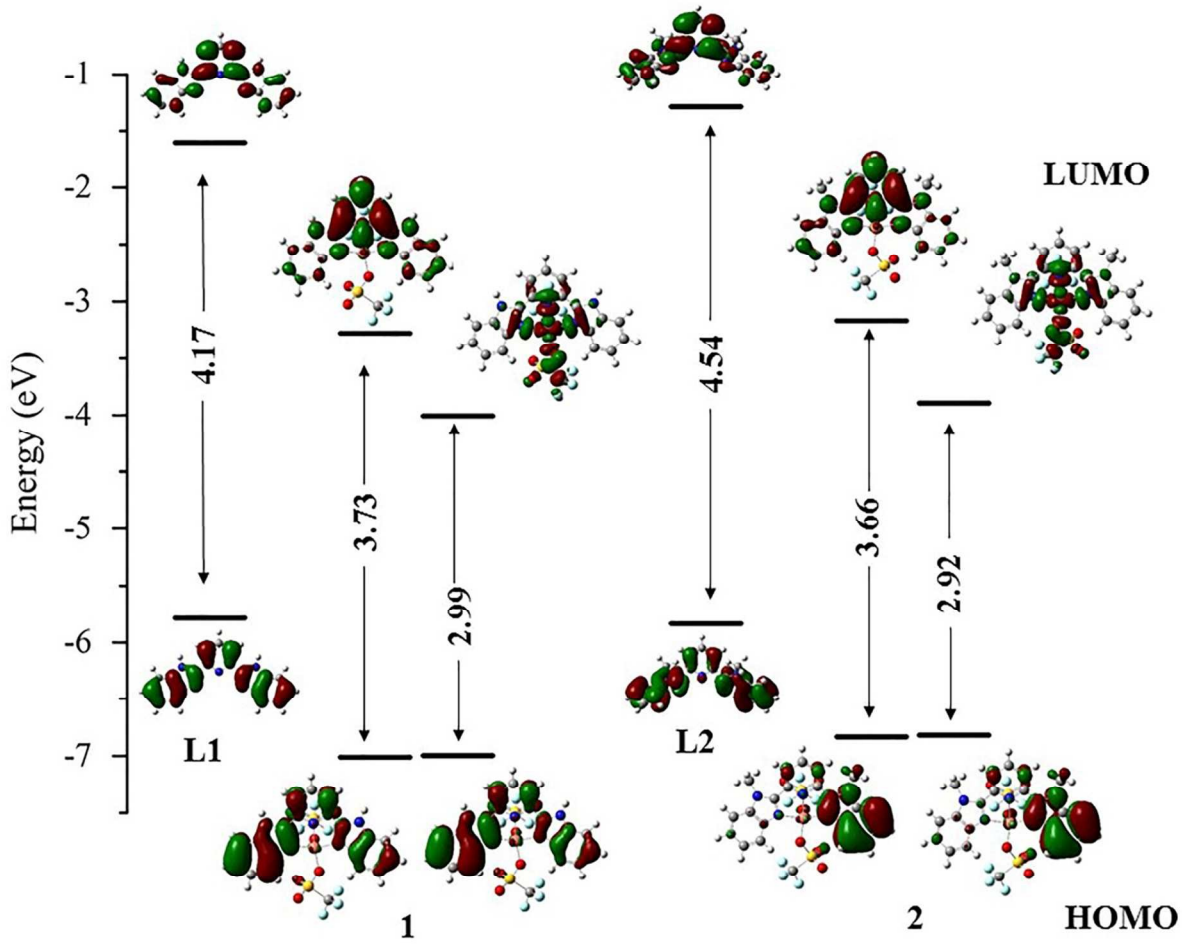

Figure 4. Energy profile diagram for L1, **1**, L2 and **2**; HOMO and LUMO are calculated by TD-DFT using B3LYP 6-31G/LANL2DZ level.

View Article Online
DOI: 10.1039/C7DT01895A

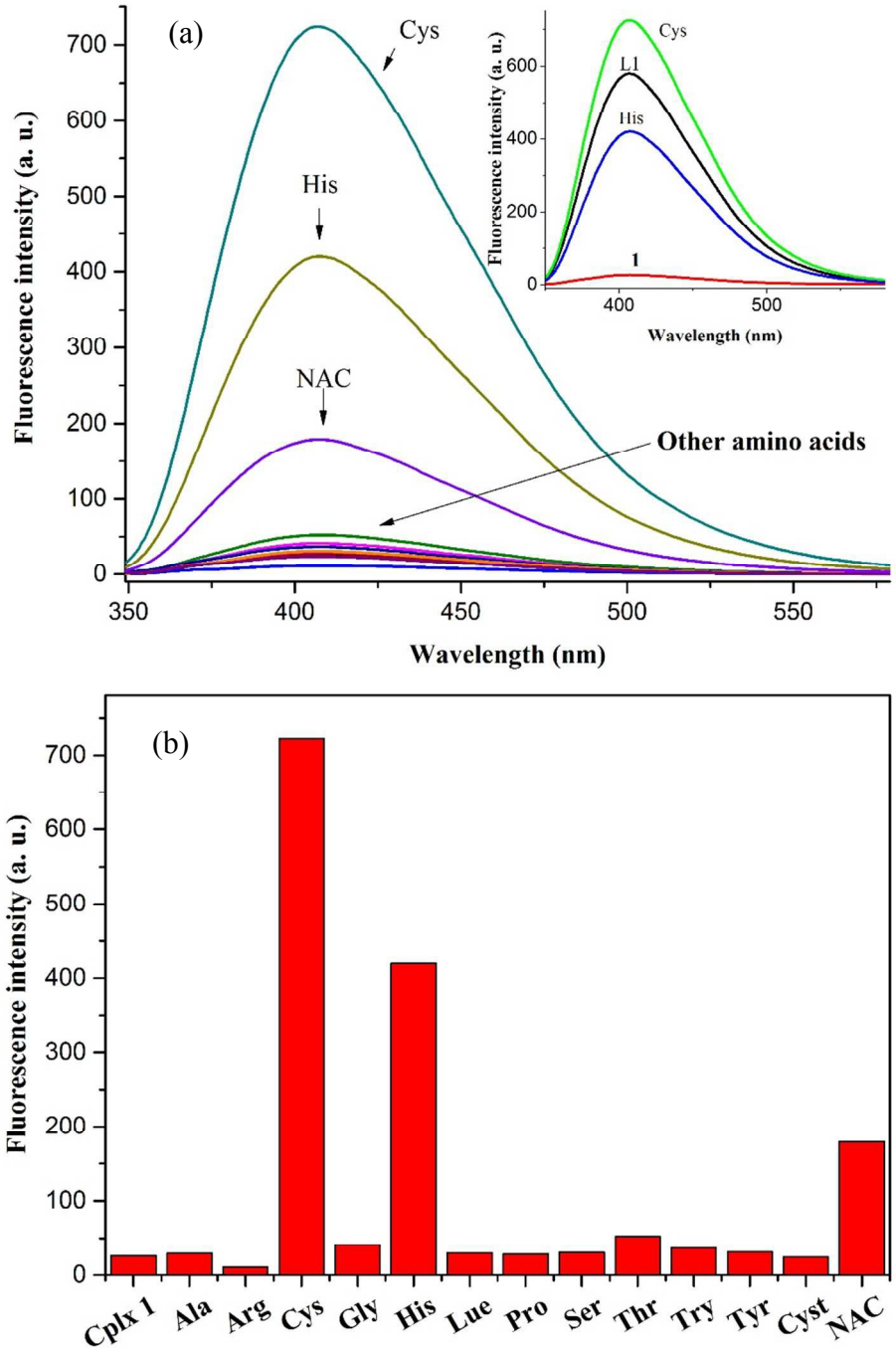

Figure 5. Fluorescence spectra of **1** and addition of various amino acids (20 equivalents) in HEPES buffer pH, at 7.34 at 25°C (5×10^{-6} M), insert: Fluorescence spectra comparison of L1, **1**, **1** + Cys and **1** + His (a). Bar diagram for the selectivity of various amino acids (λ_{ex} = 327 nm, slits: 5nm/5nm) (b).

View Article Online
DOI: 10.1039/C7DT01895A

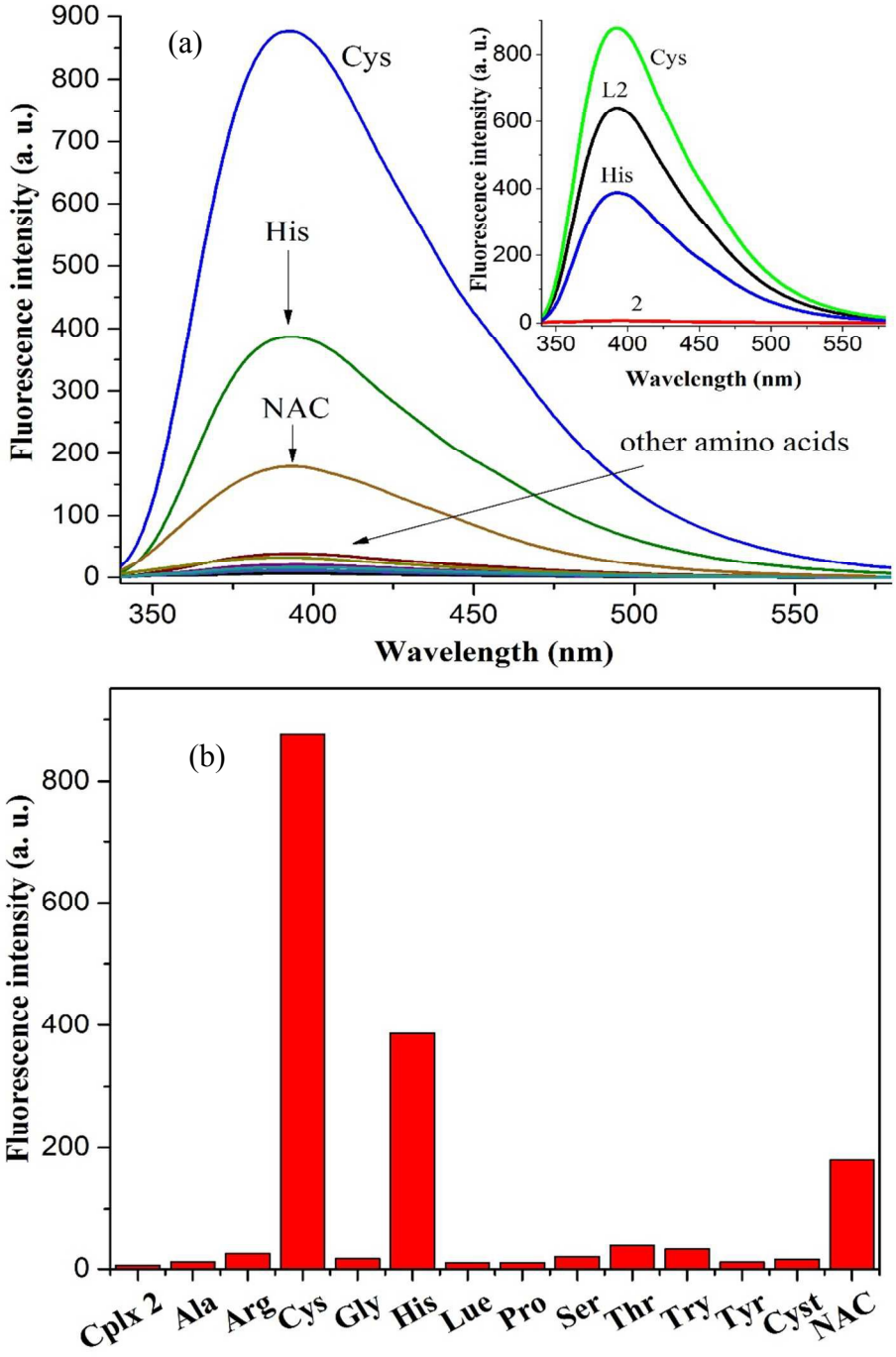

Figure 6. Fluorescence spectra of **2** and addition of various amino acids (20 equivalents) in HEPES buffer pH, 7.34 at 25°C (5×10^{-6} M). Inset: Fluorescence comparison plot of L1, **2**, **2**+ Cys and **2**+ His (a). Bar diagram for the selectivity of various amino acids (λ_{ex} = 313 nm, slits: 5nm/5nm) (b).

View Article Online
DOI: 10.1039/C7DT01895A

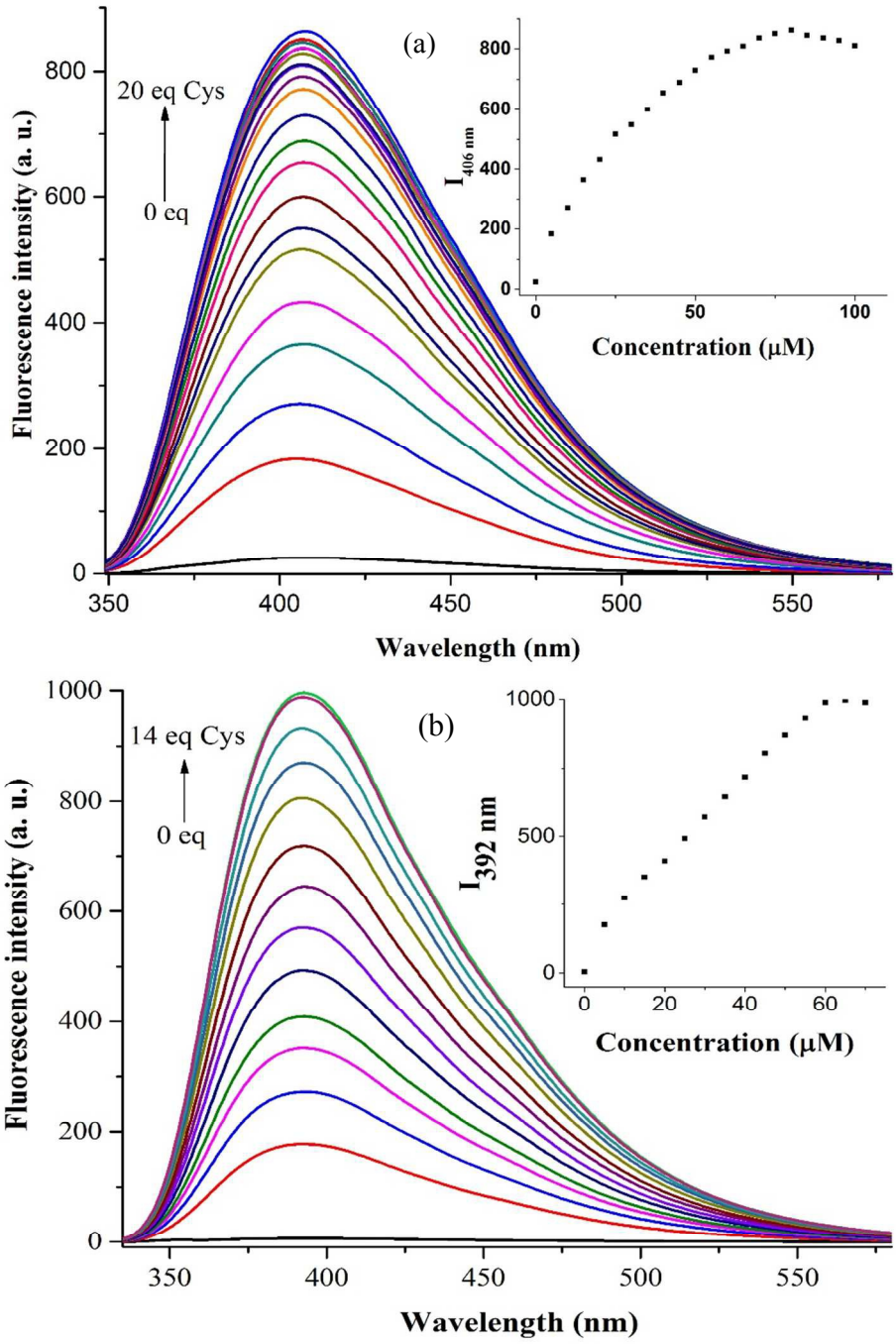

Figure 7. Fluorescence spectra of **1** (a) and **2** (b) and the addition of various equivalents of Cys in HEPES buffer solution pH, 7.34 at 25°C (5×10^{-6} M). Insets: Saturation plots.

View Article Online
DOI: 10.1039/C7DT01895A

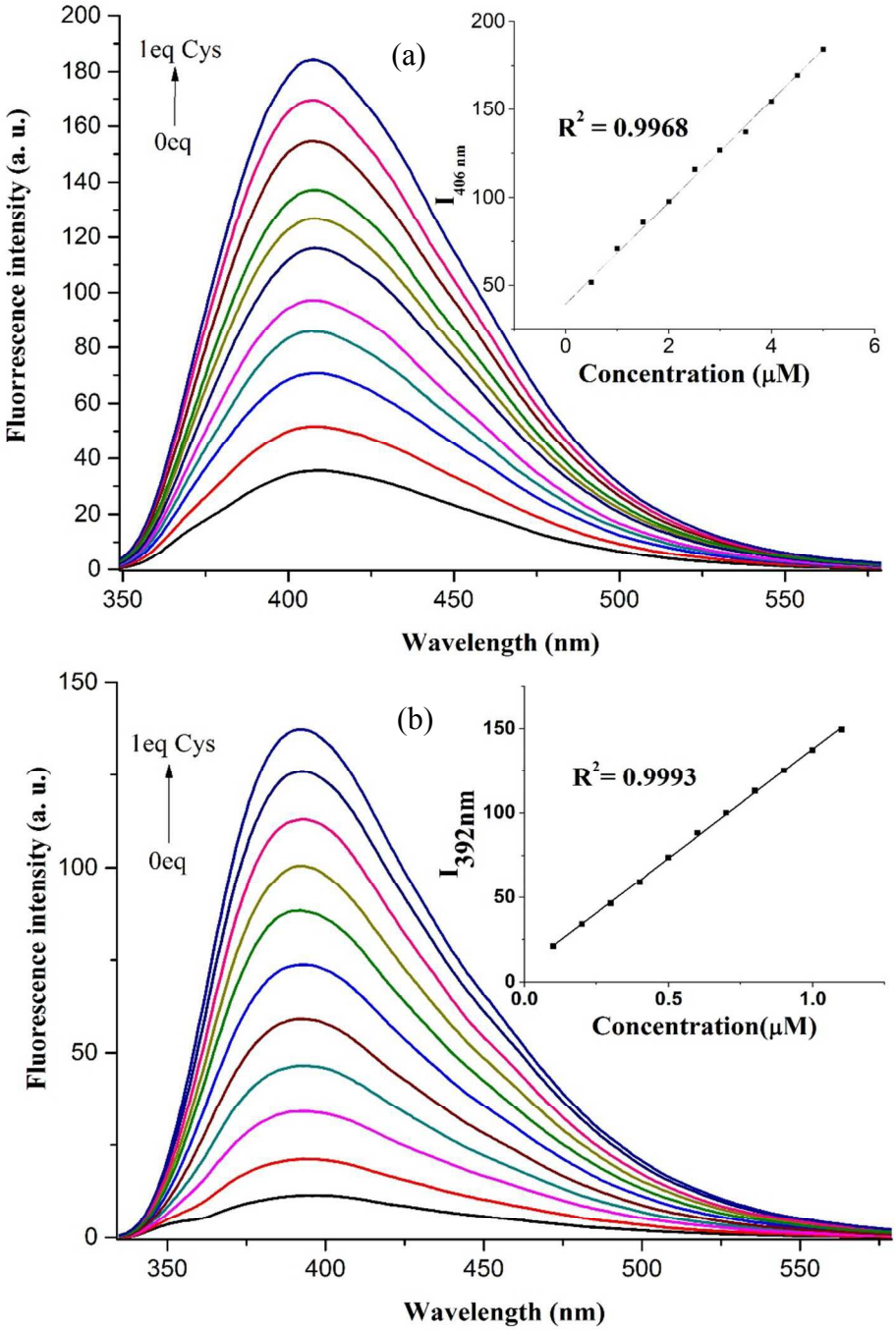

Figure 8. Fluorescence intensity changes of **1** (5×10^{-6} M) (a) and **2** (5×10^{-6} M) (b) on addition of Cys (concentration) in pH 7.34.

View Article Online
DOI: 10.1039/C7DT01895A

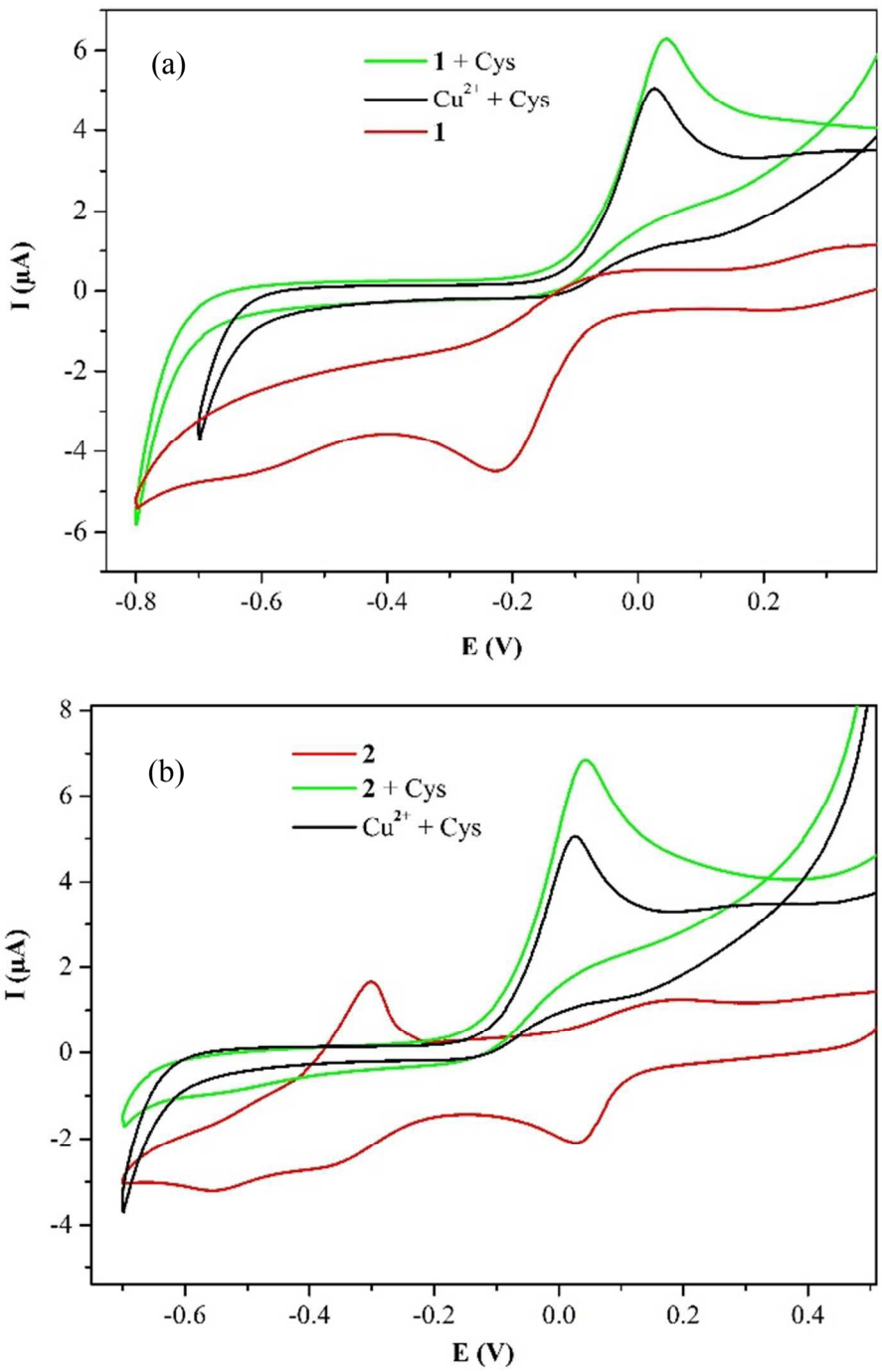

Figure 9. Cyclic voltamagrams of **1** (a), (concentration) and **2** (b) (concentration) with Cys (5×10^{-6} M) in HEPES buffer (pH 7.34) at 25°C [reference: saturated Ag/Ag^{+}; supporting electrolyte: 0.1M NaCl solution; scan rate: = 50 mV s^{-1}].

View Article Online
DOI: 10.1039/C7DT01895A

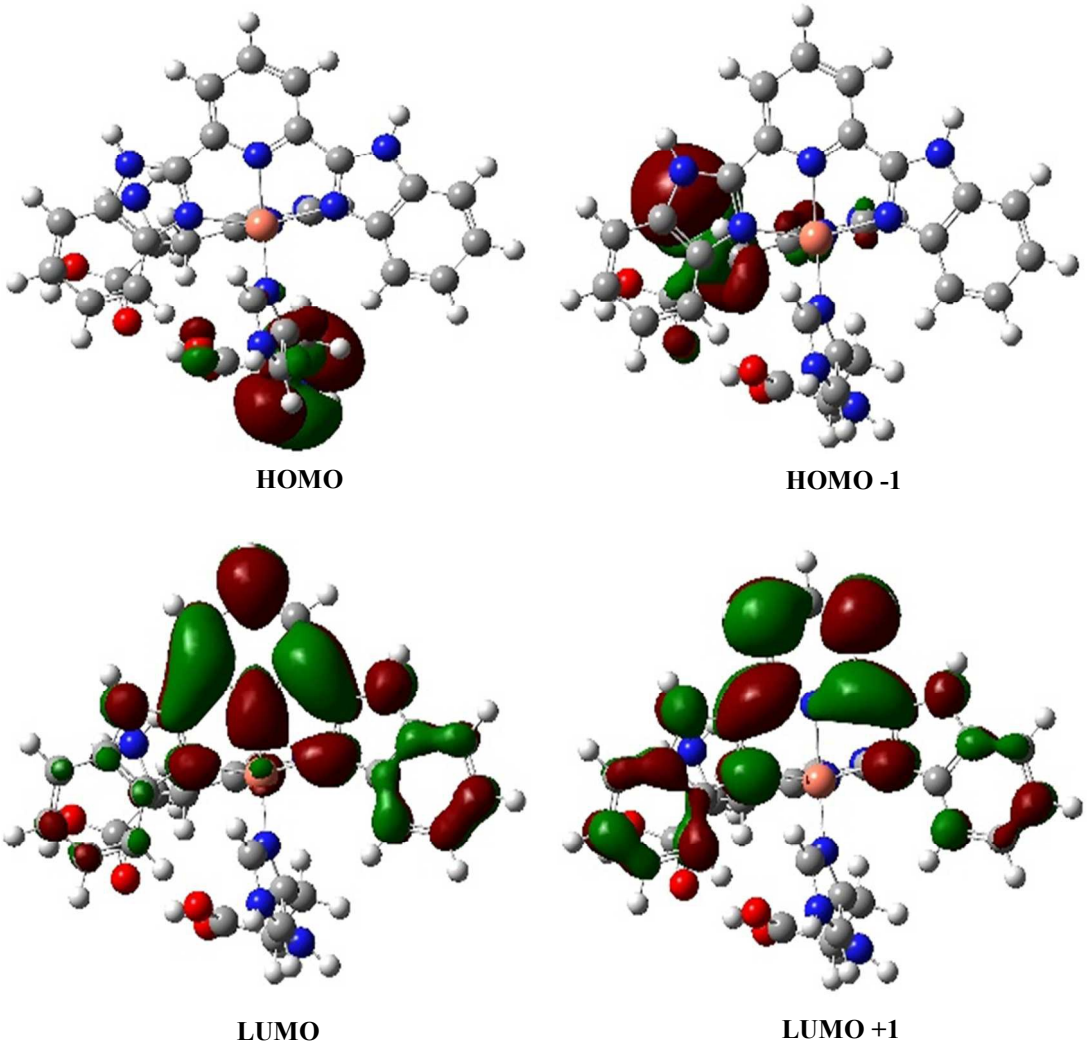

Figure 10. Frontier orbitals of **1** with His calculated using B3LYP 6-31G/LANL2DZ level.

View Article Online
DOI: 10.1039/C7DT01895A

Table 1. Crystal data and structure refinement and selected bond length (Å) and bond angles (°) of **2**

		Bond lengths and Bond angles[c]	
Empirical formula	C23 H21 Cu F6 N5 O8 S2		
FW	737.11	Cu(1)-O(1)	1.953(3)
Crystal system	Triclinic	Cu(1)-O(2)	2.247(3)
space group	P -1	Cu(1)-N(4)	1.995(4)
a (Å)	12.7225(6)	Cu(1)-N(3)	1.958(4)
b (Å)	15.1150(6)	Cu(1)-N(1)	2.000(4)
c (Å)	17.1761(7)		
α (deg)	85.831(3)		
β (deg)	68.352(4)	O(1)-Cu(1)-O(2)	91.82(14)
γ (deg)	71.152(4)	O(1)-Cu(1)-N(1)	101.37(17)
V (Å3)	2901.3(2)	O(1)-Cu(1)-N(3)	173.18(15)
T (K)	100.15	O(1)-Cu(1)-N(4)	97.55(17)
Cu Kα λ, (Å)	1.54184	N(1)-Cu(1)-O(2)	99.71(16)
Density	1.687(Mg/m^3)	N(1)-Cu(1)-N(4)	157.94(17)
Z	4	N(3)-Cu(1)-O(2)	94.55(14)
μ (mm^{-1})	3.278	N(3)-Cu(1)-N(1)	79.95(17)
F(000)	1492	N(3)-Cu(1)-N(4)	79.95(17)
Crystal size	0.07 × 0.05 × 0.05 mm^3	N(4)-Cu(1)-O(2)	90.87(15)
no. of reflections collected	10923		
GOF on F^2	1.043		
R1[a]	0.0841		
wR2[b]	0.2377		

(a) $R1 = \Sigma||Fo| - |Fc||/\Sigma|Fo|$. (b) $wR2 = [\Sigma w(Fo^2 - Fc^2)^2/\Sigma w(Fo^2)^2]^{1/2}$. [c] Standard deviations in parentheses.

View Article Online
DOI: 10.1039/C7DT01895A

Table 2. Electronic spectral, redox and computational data

	L1	**1**	**1** + Cys	**1** + His	**L2**	**2**	**2** + Cys	**2** + His
Absorption spectra[a] λ_{max} (nm), (ε, M^{-1} cm^{-1})	309 (11,480) 327 (13,020)	314 (19,740) 356 (13,180) 662 (90)*	309 (16,660) 327 (18,860)	323 (13,980) 378 (1440)	313 (10,360)	313 (16,860) 360 (9560) 651 (84)*	313 (18,760)	313 (18,580) 370 (2060)
Electrochemical data[b]								
E_{pa} (V)		-0.3129		-0.2189		-0.55 0.007		-0.4891 -0.235
E_{pc} (V)		-0.0696	0.1113	-0.3036 -0.0445		-0.3181 0.1525	0.0405	-0.3347 -0.02
$E_{1/2}$(V)		-0.1908		-0.1314		-0.434 0.0797		-0.4119 -0.1275
ΔE (mV)		243		174		232 146		154 215
EPR spectra[c]								
g value $g_{\|}$ $g_{\perp}$		2.29 2.05				2.29 2.06		
$A_{\|}$ (cm^{-1})		124×10^{-4}				156×10^{-4}		
Computational details[d] (eV)								
Optimized energy	-2.7365×10^4	-6.3894×10^4			-2.9505×10^4	-6.6033×10^4		
HOMO	-5.783	-7.011(α spin) -5.363 (β spin)			-5.835	-6.831(α spin) -6.817(β spin)		
LUMO	-1.605	-3.275 (α spin) -4.007 (β spin)			-1.287	-3.166(α spin) -3.895(β spin)		
Energy gap	4.177	3.735 (α spin) 2.99 (β spin)			4.547	3.665 (α spin) 2.922 (β spin)		
		TD-DFT						
Optimized energy	-2.7365×10^4	-6.3894×10^4			-2.9504×10^4	-6.6033×10^4		
HOMO	-5.783	-7.011 (α spin) -6.997 (β spin)			-5.835	-6.831 (α spin) -6.817 (β spin)		
LUMO	-1.605	-3.275 (α spin) -4.007 (β spin)			-1.287	-3.166 (α spin) -3.895 (β spin)		
Energy gap	4.177	3.735 (α spin) 2.99 (β spin)			4.547	3.665 (α spin) 2.922 (β spin)		

[a]Concentration of 5×10^{-6} M in HEPES buffer (pH 7.34) at 25°C.
*Concentration of 1×10^{-2} M in HEPES buffer (pH 7.34) at 25°C.
[b]Concentration of 5×10^{-6} M in HEPES buffer (pH 7.34) at 25°C.
[reference: saturated Ag/Ag^+; supporting electrolyte: 0.1M NaCl solution; scan rate: = 50 mV s^{-1}]. To convert $E_{1/2}$ vs NHE add +0.205 V.
[c]Methanol/DMF mixture at 70 K .
[d]DFT method using B3LYP 6-31G (for C, H and N)/LANL2DZ (for Cu) basis set in Gaussian 09 program.

View Article Online
DOI: 10.1039/C7DT01895A

Table of content

The copper(II)-benzimidazole complexes detect L-cysteine over other natural amino acids at pH, 7.34 by 'turn-on' fluorescence mechanism via reduction of Cu(II) to Cu(I) followed by displacement with excellent selectivity.